

The Hubble Tarantula Treasury Project

E. Sabbi and the HTTP Team

Space Telescope Science Institute – 3700 San Martin Dr. 21218, Baltimore, MD USA
e-mail: sabbi@stsci.edu

Abstract. We present results from the Hubble Tarantula Treasury Project (HTTP), a Hubble Space Telescope panchromatic survey (from the near UV to the near IR) of the entire 30 Doradus region down to the sub-solar ($\sim 0.5 M_{\odot}$) mass regime. The survey was done using the Wide Field Camera 3 and the Advanced Camera for Surveys in parallel. HTTP provides the first rich and statistically significant sample of intermediate- and low-mass pre-main sequence candidates and allows us to trace how star formation has been developing through the region. We used synthetic color-magnitude diagrams (CMDs) to infer the star formation history of the main clusters in the Tarantula Nebula, while the analysis of the pre-main sequence spatial distribution highlights the dual role of stellar feedback in quenching and triggering star formation on the giant HII region scale.

Key words. galaxies: star clusters: individual (30 Doradus, NGC2070, NGC2060, Hodge 301) – Magellanic Clouds – stars: formation – stars: massive – stars: pre-main sequence stars: evolution – stars: massive – stars: pre-main sequence

1. Introduction

The Tarantula Nebula (also known as 30 Doradus, hereafter “30 Dor”) is one of the most famous objects in astronomy. The first astronomical references to the Tarantula Nebula are more than 150 years old (de la Caille 1761; Herschel 1847). For more than a decade Tarantula’s ionizing cluster, Radcliffe 136 (R136), was thought to be the most massive known single star ($250 - 1000 M_{\odot}$; Feitzinger et al. 1980). Apart from a few dissonant voices (e.g., Feast 1953; Walborn 1973; Moffat 1982), the true nature of R136 continued to elude the majority of the astronomical community until Weigelt & Baier (1985) resolved it into eight components by using holographic speckle interferometry.

30 Dor is the most powerful source of H α emission in the Local Group ($f(H\alpha) \sim$

$1.3 \times 10^{-8} \text{ erg cm}^{-2} \text{ s}^{-1}$, Kennicutt & Hodge 1986). Located in the Large Magellanic Cloud (LMC), 30 Dor is the closest extragalactic giant HII region, and is comparable in size ($\sim 200 \text{ pc}$ in diameter) to the unresolved luminous HII complexes observed in distant galaxies (Oey et al. 2003; Hunt & Hirashita 2009).

R136 hosts the most massive stars known so far (Crowther et al. 2010; Bestenlehner et al. 2011), and is considered a testbed for understanding the early evolution of massive stars. Tarantula’s density of OB stars parallel those observed in systems characterized by very intense star formation, such as the starburst knots observed in interacting galaxies in the local universe and young galaxies at high redshift ($z > 5$; Meurer et al. 1997; Shapley et al. 2003; Heckman et al. 2004), and is considered one of the few known starbursts in the Local Group.

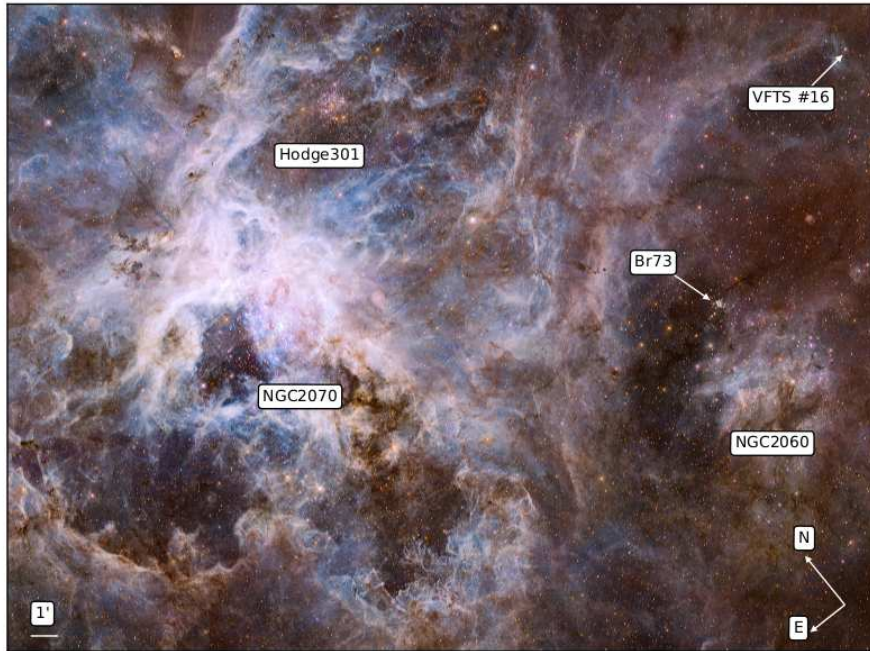


Fig. 1. Color-composite image of the Tarantula Nebula in the light of F275W and F336W (in blue), F658N (in green) and F775W (in red). Positions of the four main clusters and associations are highlighted as well as the position of the candidate run-away star VFTS-16.

Here we present results from the ‘‘Hubble Tarantula Treasury Project’’ (HTTP, PI: Sabbi, GO-12939; Sabbi et al. 2013, 2016) a treasury program designed to observe the entire 30 Doradus region with the Hubble Space Telescope (HST) in the near-ultraviolet (NUV, F275W and F336W), optical (F555W, F658N), and near-infrared (NIR, F110W and F160W). The program was built on an existing HST monochromatic survey in the F775W filter (GO-12499, PI: Lennon), designed to measure proper motions of runaway candidates (Platais et al. 2015).

A color-composite image of the entire region surveyed by HTTP is shown in Figure 1. The position of the main clusters and associations is highlighted for reference.

2. Stellar populations in the Tarantula Nebula

We used HTTP color-magnitude diagrams (CMDs) to interpret the stellar populations

found in 30 Doradus. Figure 2 shows the m_{F110W} versus $m_{F110W} - m_{F160W}$ CMD at the NIR wavelengths. Because the older stars in the CMD belong to the field of the LMC, this diagram can be used to study the properties of the stellar populations that formed in the region during the LMC’s lifetime.

The brighter ($m_{F110W} > 18$) and bluer ($m_{F110W} - m_{F160W} < 0.2$) stars in Figure 2 are young massive main sequence (MS) stars. Massive stars are short-lived objects that can be used to highlight sites of recent star formation. Figure 3 shows the spatial distribution of the high-mass stars candidates superimposed on the 30 Doradus mosaic obtained in the filter F555W. The size of the circles is proportional to the apparent magnitude of the stars, with the larger symbols corresponding to the brighter sources, while the colors represent the color excess due to dust extinction. The majority of the faint ($m_{F110W} < 18$) and red ($m_{F110W} - m_{F160W} > 0.16 * m_{F110W} - 3$)

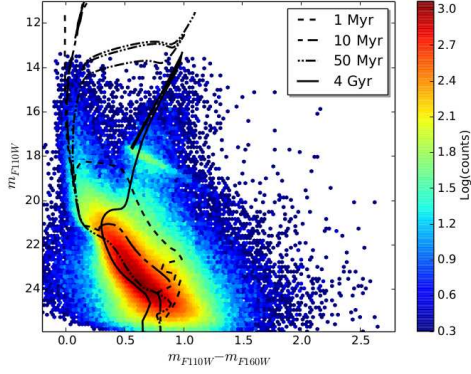


Fig. 2. NIR m_{F110W} vs. $m_{F110W} - m_{F160W}$ CMD for the entire region covered by HTTP. Padova isochrones for metallicity $Z = 0.008$ and ages = 1, 10, and 25 Myr are superimposed using black dashed, short-dashed-long-dashed, and dashed-dotted-dotted lines respectively. The continuous black line corresponds to a 4 Gyr old isochrone with metallicity $Z = 0.004$. For all isochrones, we assumed a distance modulus of 18.5. To fit the bluer edge of the younger (≤ 500 Myr old) stellar populations, in addition to the Galactic extinction ($R_V = 3.1$ and $A_V = 0.06$), a minimum $E(B - V) = 0.3$ was needed. Extinction coefficients $A_{F110W} = 1.9$ and $A_{F160W} = 1.3$ are from De Marchi et al. (2016). The Galactic foreground extinction was sufficient to fit the bluer edge of the red clump.

stars are likely low-mass young pre-main sequence (PMS) stars, that are not yet burning hydrogen in their core. Because of their young age, PMS stars have not had time to migrate far away from their birth place, and therefore their spatial distribution can be used to trace how star formation occurred across a region. For this purpose, we selected all the sources that in Figure 2 to the right of the Padova $Z = 0.008$ 5Myr old isochrone (assuming the distance modulus 18.5 and $E(B - V) = 0.3$), in the magnitude range $21.5 < m_{F110W} < 23.0$.

PMS candidates can be found almost everywhere in the region (see also Figure 4 in and Figure 22 in Cignoni et al. 2015; Sabbì et al. 2016, respectively), although clear overdensities can be noted, for example, in correspondence of the two young clusters NGC 2060 and NGC 2070. Because highly extinguished MS

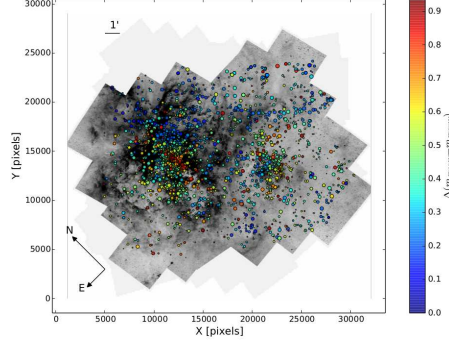


Fig. 3. Spatial distribution of the massive stars overlaid on the image of 30 Doradus obtained in the ACS filter F555W. The size of the circles relates to the luminosity of the sources. Stars are color-coded according to their color excess due to dust extinction.

and SGB stars can contaminate the distribution of PMS candidates, in Figure 4 we show the density contours only for regions whose number of PMS candidates is above the 50 percentile. This selection allows us also to highlight the clustering properties of these sources (Lada & Lada 2003). To help with the interpretation in the upper panel, we superimposed the density contours on the mosaic acquired in the F555W filter. The figure shows an excellent correlation between the distribution of the PMS candidates and the ionized filaments of ionized gas and warm dust that envelope and confine several extended hot ($10^6 - 10^7$ K) bubbles of plasmas. In particular we find the following:

- To the north, chains of small clusters clearly depart from NGC 2070 and envelop a giant hot super bubble. The densest point in this system is only partially resolved into stars by HST and is still heavily embedded in its dusty cocoon. This system, nicknamed the "Skull Nebula," is also one of the brightest sources in mid-IR (Walborn et al. 2013).
- Several clumps of PMS candidates surround the large cavities to the South-East of NGC 2070.
- PMS stars surround NGC 2060. The two richer systems coincide with diffuse soft X-

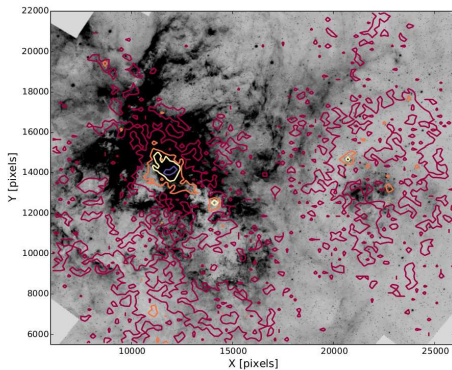


Fig. 4. Spatial distribution of PMS star candidates younger than 5 Myr overlaid on the image of 30 Doradus obtained in the ACS filter F555W.

rays to the north and the east of the SNR, the larger being associated with the compact bright cluster hosting Br73.

- The large arc of gas and dust that divides NGC 2060 and NGC 2070 is the birthsite of several compact associations.
- The clumps of PMS candidates identified with HTTP also correlate with the population of embedded young stellar objects (YSOs) identified by Seale et al. (2014) combining Herschel and Spitzer data.

The strong correlation between cool gas, warm dust, and PMS candidates, as well as the anti-correlation between hot gas and very recent star formation is an observational demonstration of how, by carving cavities in the ISM, strong stellar winds from massive stars, WR stars, and supernovae explosions, shut down star formation (disruptive feedback) in some regions, and ignite new generations of stars several parsecs away, (constructive feedback Sabbi et al. 2016).

3. The star formation history of the two main star clusters in 30 Dor

30 Doradus allows us to study the process star formation on a variety of scales and stellar densities, from the dense cluster R 136, possibly a newborn globular cluster, via the massive star-forming region NGC 2070, the "old"

(26.5–31.5 Myr Cignoni et al. 2016) populous cluster Hodge 301, to the many diffuse star-forming regions like NGC 2060. Deciphering the history of 30 Doradus is therefore a unique opportunity to understand how star formation originates and propagates.

In order to recover the SFH of the main clusters in 30 Doradus, we had to face three major problems:

- Severe crowding conditions that strongly limit the completeness of our data, and reduce shortening the look-back time;
- The contamination from stars belonging to the field of the LMC, that would mimic a prolonged star formation;
- The high level of differential reddening that broadens and dims the CMD, blending together young PMS stars and older MS stars, which introduces further age ambiguities.

We used extensive artificial star testing experiments to obtain reliable estimates of photometric errors and completeness. In order to minimize the contamination from the LMC field, we carefully selected a region in the Tarantula Nebula that showed minimal differential reddening, negligible SF activity in the last 50 Myr and high completeness down to $m_{F555W} = 24$. We then artificially corrected this reference field for the more severe incompleteness and photometric errors typical of other regions. We then normalized the field to the stellar densities found in the analyzed region and applied corrections for differential reddening.

3.1. Star formation history of NGC 2070

We used synthetic CMDs to recover the star formation history (SFH) of the starbursting region NGC 2070. This technique was originally developed by Tosi et al. (1991) and, after undergoing several improvements and refinements, can now provide reliable SFHs for any resolved population within ≈ 20 Mpc (see, e.g. Tolstoy et al. 2009, and references therein).

Our analysis indicates that NGC 2070 experienced prolonged activity. The first significant period of SF started about ≈ 20 Myr ago.

SF then accelerated throughout the entire region about 7 Myr ago. Between 1 and 3 Myr ago the SF activity reached a peak. In this time range, the SF moved from the periphery to the central regions.

In the innermost 20 pc NGC 2070 formed $\approx 8.7 \times 10^4 M_{\odot}$. Except in the innermost few parsecs, where the incompleteness is too severe to allow firm conclusions, in the range $0.5 - 7 M_{\odot}$ a Kroupa initial mass function is compatible with the data. To the level we can measure, low-mass stars can form in starburst regions in the same way they form in low-density environments. At high masses, our synthetic CMDs tend to underestimate the star counts in the densest regions. This may suggest a flattening of the IMF above $10 M_{\odot}$. (Cignoni et al. 2015).

3.2. Star formation history of Hodge 301

From a comparison of the observed CMD with simulations based on stellar evolutionary models we also derive the age distribution and reddening of Hodge 301. The peak age derived from fitting the PMS turn on and the MS turn off is between 26.5 and 31.5 Myr, considerably older than the bulk of the stars in NGC 2070, but only slightly older than NGC 2070 oldest stars.

H301s total stellar mass is $\sim 8800 \pm 800 M_{\odot}$ and in the region there have likely been between 38 and 61 Type-II supernovae explosions. From the point of view of the Tarantula Nebula, the old age of Hodge 301, several Myr older than the nearby and massive NGC 2070, and its high supernovae activity, along with the fact that no older clusters are visible in the region, could suggest that the onset of Hodge 301 sparked the formation of NGC 2070 (Cignoni et al. 2016).

4. Summary and conclusions

HTTP (HST GO-12939, PI: E. Sabbi) is a multi-wavelength study of 30 Doradus, the closest extragalactic giant HII region and an excellent example of large-scale star formation in an environment that, in many ways (such

as metallicity, dust content and SF rate), resembles the extreme conditions of the early universe. HTTP covers the 30 Dor region in the NUV (F275W, F336W), optical (F555W, F658N, F775W), and NIR (F110W, F160W) wavelengths using simultaneously both the imagers (WFC3 and ACS) currently operating on HST. More information about the HTTP project can be found in Sabbi et al. (2013, 2016) and from the url <https://archive.stsci.edu/prepds/30dor/index.html>. Astrophotometric catalog and drizzled mosaics can be downloaded from <https://archive.stsci.edu/prepds/30dor/Preview/observations.html>.

Our study probes the stellar content of the Tarantula Nebula down to $\sim 0.5 M_{\odot}$ and provides a snapshot of the history of star formation of the entire region, confirming that 30 Dor is a complex region that has built up its stellar content over several million years. While several studies have focused on Tarantulas massive stars, HTTP has provided for the first time a rich and statistically significant census of the low-mass PMS stars. Although the complicated kinematics (Chu & Kennicutt 1994) and the highly variable reddening make it difficult to infer the tridimensional structure of 30 Dor, the high spatial resolution and sensitivity of HST have allowed us to trace how star formation has been developing in the region.

The distribution of UMS stars and PMS candidates in clumps and filaments mimics the predictions of recent hydrodynamical simulation (i.e., Bate 2012; Krumholz et al. 2012; Schneider et al. 2012), supporting the hypothesis that stars may preferentially form in those filaments of gas that built up more mass during the turbulent formation of the cloud. In addition, the fact that PMS candidates surround many of the super-bubbles carved by supernova explosions suggests that fast supernova explosions had a major role in triggering the most recent episodes of star formation and that stellar feedback is still shaping the region. The overlap between PMS candidates and embedded YSOs indicates that, once initiated, the process of star formation continues for at least a few million years, even in the presence of fast stellar winds and high UV radiation, and that

the SF episode in 30 Dor is not complete and is continuing to evolve.

References

- Bate, M. R. 2012, *MNRAS*, 419, 3115
- Bestenlehner, J. M., Vink, J. S., Gräfener, G., et al. 2011, *A&A*, 530, L14
- Cignoni, M., Sabbi, E., van der Marel, R. P., et al. 2015, *ApJ*, 811, 76
- Cignoni, M., Sabbi, E., van der Marel, R. P., et al. 2016, *ApJ*, 833, 154
- Chu, Y.-H., & Kennicutt, R. C., Jr. 1994, *AJ*, 108, 1696
- Crowther, P. A., Schnurr, O., Hirschi, R., et al. 2010, *MNRAS*, 408, 731
- de la Caille, N. L. 1761, *Philosophical Transactions*, 52, 21
- De Marchi, G., Panagia, N., Sabbi, E., et al. 2016, *MNRAS*, 455, 4373
- Feast, M. W. 1953, *The Observatory*, 73, 255
- Feitzinger, J. V., et al. 1980, *A&A*, 84, 50
- Heckman, T. M., Kauffmann, G., Brinchmann, J., et al. 2004, *ApJ*, 613, 109
- Herschel, J. F. W. 1847, *Results of Astronomical Observations made during the Years 1834*, 5, 6, 7, 8, at the Cape of Good Hope; Being the Completion of a Telescopic Survey of the Whole Surface of the Visible Heavens, Commenced in 1825 (Smith, Elder and Co., Cornhill, London)
- Hunt, L. K., & Hirashita, H. 2009, *A&A*, 507, 1327
- Kennicutt, R. C., & Hodge, P. W. 1986, *ApJ*, 306, 130
- Krumholz, M. R., Klein, R. I., & McKee, C. F. 2012, *ApJ*, 754, 71
- Lada, C. J., & Lada, E. A. 2003, *ARA&A*, 41, 57
- Meurer, G. R., et al. 1997, *AJ*, 114, 54
- Moffat, A. F. J. 1982, *JRASC*, 76, 323
- Oey, M. S., et al. 2003, *AJ*, 126, 2317
- Platais, I., van der Marel, R. P., Lennon, D. J., et al. 2015, *AJ*, 150, 89
- Sabbi, E., Anderson, J., Lennon, D. J., et al. 2013, *AJ*, 146, 53
- Sabbi, E., Lennon, D.J., Anderson, J., et al. 2016, *ApJS*, 222, 11
- Schneider, N., Csengeri, T., Hennemann, M., et al. 2012, *A&A*, 540, L11
- Seale, J. P., Meixner, M., Sewilo, M., et al. 2014, *AJ*, 148, 124
- Shapley, A. E., et al. 2003, *ApJ*, 588, 65
- Tolstoy, E., Hill, V., & Tosi, M. 2009, *ARA&A*, 47, 371
- Tosi, M., et al. 1991, *AJ*, 102, 951
- Walborn, N. R. 1973, *ApJ*, 182, L21
- Walborn, N. R., Barba, R. H., & Sewilo, M. 2013, *AJ*, 145, 98
- Weigelt, G., & Baier, G. 1985, *A&A*, 150, L18